Progress of Theoretical Physics, Vol. 126, No. 6, December 2011

Constraints from Unrealistic Vacua in the Next-to-Minimal Supersymmetric Standard Model

Yoshimi KANEHATA,[1,2,*)] Tatsuo KOBAYASHI,[3,**)] Yasufumi KONISHI,[1,***)]
Osamu SETO[4,†)] and Takashi SHIMOMURA[5,††)]

[1]*Maskawa Institute for Science and Culture, Kyoto Sangyo University, Kyoto 603-8555, Japan*
[2]*Department of Physics, Ochanomizu University, Tokyo 112-8610, Japan*
[3]*Department of Physics, Kyoto University, Kyoto 606-8502, Japan*
[4]*Department of Architecture and Building Engineering, Hokkai-Gakuen University, Sapporo 062-8605, Japan*
[5]*Yukawa Institute for Theoretical Physics, Kyoto University, Kyoto 606-8502, Japan*

(Received October 14, 2011)

We study constraints to avoid deep unrealistic minima in the next-to-minimal supersymmetric standard model. We analyze the scalar potential along directions where all of and one of the three Higgs fields develop their vacuum expectation values, and find unrealistic minima deeper than the electroweak symmetry breaking (EWSB) vacuum. These unrealistic minima threaten the realization of successful EWSB and therefore should be avoided. Necessary conditions for avoiding these minima result in constraints on parameters. We show that a wide and significant region of the parameter space, especially a large λ, is ruled out by our constraints.

Subject Index: 113

§1. Introduction

The origin of the electroweak (EW) scale and its stability against large radiative corrections are unanswered questions in the standard model (SM) of elementary particles. New physics beyond the SM should provide a solution for stabilizing its scale. Supersymmetry (SUSY) is one of the promising frameworks in this regard. The simplest supersymmetric extension of the SM is the minimal supersymmetric standard model (MSSM).

The MSSM suffers from a naturalness problem, the so-called μ problem.[1)] The MSSM has a supersymmetric Higgs/Higgsino mass term, the μ term, with a dimensionful parameter μ. Although μ is usually assumed to be on the order of the EW scale, there is no a priori reason for this. If μ was much larger than the EW scale, new fine-tuning would be reintroduced to obtain the observed masses of gauge bosons.

*) E-mail: yoshimi@cc.kyoto-su.ac.jp
**) E-mail: kobayash@gauge.scphys.kyoto-u.ac.jp
***) E-mail: konishi@cc.kyoto-su.ac.jp
†) E-mail: seto@physics.umn.edu
††) E-mail: stakashi@yukawa.kyoto-u.ac.jp

On the other hand, if μ was much smaller than the EW scale, it would conflict with the nonobservation of a new charged fermion, namely, the charged Higgsino.

The next-to-minimal supersymmetric standard model (NMSSM)[2)–10)] (for a review, see 11)) is the simplest extension of the MSSM by adding one gauge singlet superfield $\hat{S}$ and the $\mathbb{Z}_3$ symmetry. The μ term is forbidden by the $\mathbb{Z}_3$ symmetry; instead, it is generated effectively after the singlet scalar S develops its vacuum expectation value (vev). The singlet scalar S develops a vev associated with the standard radiative symmetry breaking at the EW scale. Hence, its vev automatically takes a value on the order of the EW scale. Another advantage of the NMSSM is related to the Higgs mass. From the nonobservation of the CP-even light Higgs boson h at LEP II, the lower bound on its mass m_h has been obtained as $m_h > 114$ GeV in the SM like Higgs.[12)] Within the MSSM, the lightest CP-even Higgs mass is bounded by the Z boson mass m_Z at the tree level. Radiative corrections due to stop (a superpartner of top quark) masses increase the Higgs mass,[13)–15)] but one may need a large stop mass such as $\mathcal{O}(1)$ TeV to make the lightest Higgs sufficiently heavier than the LEP bound. Such heavy stops would lead to a fine-tuning problem, in other words the little hierarchy problem,[16)–21),*)] which could be moderated in the NMSSM. The Higgs potential of the NMSSM has a new quartic term, which increases the lowest CP-even Higgs mass at the tree level.

Although the NMSSM has the appealing features mentioned above, the structure of the scalar potential of the NMSSM is more complicated than that of the MSSM owing to the presence of an additional singlet scalar S. As far as the NMSSM scalar potential is concerned, the cosmological domain wall problem caused by the symmetries of the NMSSM has been well studied.[32),33)] The domain wall problem can be avoided by introducing suitable non-renormalizable operators that do not generate a dangerously large tadpole.[34)–36)] However, this is not the end of the story. Since the potential is complicated, phenomenologically unacceptable vacua could exist. Hence, it is important to analyze the vacuum structure of the Higgs scalar potential, and to derive conditions for avoiding unrealistic minima and realize successful EW symmetry breaking (EWSB). Such studies would provide us with significant constraints on the parameter space of couplings and soft SUSY breaking terms in the NMSSM. In fact, several studies have been performed on the structure of vacua, e.g., by numerical analysis with one-loop corrections.[37)–39)]

In addition to the Higgs scalar fields, there are other scalar fields, which are superpartners of quarks and leptons, i.e., the so-called squarks and sleptons. They might develop vevs and lead to unrealistic vacua. On such vacua, colour and/or charge breaking (CCB) may occur if squarks and sleptons develop vevs.[7),8),40)–46)] Moreover, the potential may include directions unbounded from below (UFB). Systematic studies of such unrealistic vacua and UFB directions have been carried out in the MSSM.[47)] Recently, such analyses have also been extended including terms generating nonvanishing neutrino masses and the corresponding soft SUSY breaking terms,[48),49)] and flavour physics, e.g. 50)–52). From these analyses, one can derive necessary conditions in order to avoid unrealistic vacua and realize success-

[*)] See also e.g. 22)–31).

ful EWSB which result in theoretical constraints among couplings and soft SUSY breaking terms. These constraints will be useful to eliminate the parameter space of the models, and hence are important. Our purpose in this paper is to extend such systematic analyses on unrealistic vacua to the NMSSM.

In this paper, we analyze the vacuum structure of the Higgs scalar potential in the NMSSM at the tree-level. We study unrealistic vacua and derive conditions to avoid them. We investigate the implications of these constraints by using examples of numerical analyses and by simplifying the constraints in a certain limit. We also study unrealistic vacua of scalar potential including squarks and sleptons.

This paper is organized as follows. In §2, we review the Higgs potential, EWSB vacuum and Higgs masses of the NMSSM. In §3, we study unrealistic minima and show necessary conditions to avoid them. In §4, we study our constraints numerically for several examples. Section 5 is devoted to conclusion and discussion. We give our notations and the scalar potential of the NMSSM in Appendix A. In Appendix B, we give detailed studies on the unrealistic minima, where squarks and sleptons as well as the singlet S develop their vevs in the NMSSM.

§2. Realistic vacuum of the NMSSM

The NMSSM is an extension of the MSSM, achieved by adding an extra gauge singlet scalar, S, and its fermionic partner, $\tilde{S}$. This new scalar participates in EWSB together with two doublet Higgs scalars by developing their vevs. In this section, we briefly review a realistic vacuum of the NMSSM, in which EWSB successfully occurs. Notations of particles are summarized in Appendix A.

The superpotential of the NMSSM is given by

$$\mathcal{W}_{\rm NMSSM} = Y_d \hat{H}_1 \cdot \hat{Q}\hat{D}^c_R + Y_u \hat{H}_2 \cdot \hat{Q}\hat{U}^c_R + Y_e \hat{H}_1 \cdot \hat{L}\hat{E}^c_R - \lambda \hat{S}\hat{H}_1 \cdot \hat{H}_2 + \frac{1}{3}\kappa \hat{S}^3, \quad (1)$$

where Y_u, Y_d and Y_e are the Yukawa couplings of up-type quarks, down-type quarks and charged leptons, respectively, and λ and κ are Yukawa coupling constants of the Higgs scalars. Here, we impose a global $\mathbb{Z}_3$ symmetry to forbid tadpole and quadratic terms. The soft SUSY breaking terms are given by

$$\begin{aligned} V_{\rm soft} = {}& m^2_{H_1} H^\dagger_1 H_1 + m^2_{H_2} H^\dagger_2 H_2 + m^2_S S^\dagger S - \left(\lambda A_\lambda S H_1 \cdot H_2 - \frac{1}{3}\kappa A_\kappa S^3 + \text{h.c.}\right) \\ & + m^2_{\tilde{Q}} \tilde{Q}^\dagger \tilde{Q} + m^2_{\tilde{u}_R} \tilde{u}^*_R \tilde{u}_R + m^2_{\tilde{d}_R} \tilde{d}^*_R \tilde{d}_R + m^2_{\tilde{L}} \tilde{L}^\dagger \tilde{L} + m^2_{\tilde{e}_R} \tilde{e}^*_R \tilde{e}_R \\ & + \left(A_d Y_d H_1 \cdot \tilde{Q}\tilde{d}^*_R + A_u Y_u H_2 \cdot \tilde{Q}\tilde{u}^*_R + A_e Y_e H_1 \cdot \tilde{L}\tilde{e}^*_R + \text{h.c.}\right), \end{aligned} \quad (2)$$

where we assume that all of the soft masses, trilinear couplings and Yukawa couplings are real for simplicity. Indices for the generation of squarks and sleptons are omitted. The scalar potential of the Higgs scalars can be obtained from the F- and D-terms given in Appendix A and the soft SUSY breaking terms. For the EW symmetry to be successfully broken, the neutral Higgs fields develop vevs while vevs of the charged Higgs fields are vanishing. Using the gauge transformations, without loss of generality, one can take $\langle H^+_2 \rangle = 0$ and $\langle H^0_2 \rangle = v_2 \in \mathbb{R}^+$. The condition for vanishing $\langle H_1^- \rangle$ is to require that the charged Higgs scalars have positive masses squared. Then, the Higgs potential of the neutral components is given by

$$V = \lambda^2|S|^2\left(|H_1^0|^2+|H_2^0|^2\right)+\lambda^2|H_1^0|^2|H_2^0|^2+\kappa^2|S|^4-\left(\lambda\kappa H_1^0H_2^0(S^*)^2+\text{h.c.}\right)$$
$$+\frac{1}{8}g^2\left(|H_1^0|^2-|H_2^0|^2\right)^2+m_{H_1}^2|H_1^0|^2+m_{H_2}^2|H_2^0|^2+m_S^2|S|^2$$
$$-\left(\lambda A_\lambda H_1^0H_2^0S-\frac{1}{3}\kappa A_\kappa S^3+\text{h.c.}\right), \tag{3}$$

where $g^2=g_1^2+g_2^2$, and g_1 and g_2 denote the gauge coupling constants of $U(1)$ and $SU(2)$, respectively. The Higgs sector is characterized by the following parameters:

$$\lambda,\ \ \kappa,\ \ m_{H_1}^2,\ \ m_{H_2}^2,\ \ m_S^2,\ \ A_\lambda\ \ \text{and}\ \ A_\kappa. \tag{4}$$

The remaining vevs of H_1^0 and S in general can be complex. However, in Ref. 53), it was shown that such CP violating extrema are maxima rather than minima. Thus, it is reasonable to assume that neutral Higgs fields develop real and nonvanishing vevs, whereas charged ones do not. Then, we denote vevs as

$$\langle H_1^0\rangle = v_1, \qquad \langle H_2^0\rangle = v_2, \qquad \langle S\rangle = s. \tag{5}$$

Furthermore, as was discussed in Ref. 37), the Higgs potential given by Eq. (3) is invariant under the replacements $\lambda,\ \kappa,\ s\rightarrow -\lambda,\ -\kappa,\ -s$ and $\lambda,\ v_1\rightarrow -\lambda,\ -v_1$; therefore, we can take λ and v_1 to be always positive, while κ, $\mu(\equiv\lambda s)$, A_λ and A_κ can have both signs. These vevs are determined by minimizing the potential in Eq. (3), with respect to the neutral Higgs scalars, that is, they satisfy the following stationary conditions:

$$\frac{\partial V}{\partial H_1^0} = \lambda^2 v\cos\beta(s^2+v^2\sin^2\beta)-\lambda\kappa v s^2\sin\beta+\frac{1}{4}g^2v^3\cos\beta\cos 2\beta$$
$$+m_{H_1}^2 v\cos\beta-\lambda A_\lambda v s\sin\beta=0, \tag{6a}$$
$$\frac{\partial V}{\partial H_2^0} = \lambda^2 v\sin\beta(s^2+v^2\cos^2\beta)-\lambda\kappa v s^2\cos\beta-\frac{1}{4}g^2v^3\sin\beta\cos 2\beta$$
$$+m_{H_2}^2 v\sin\beta-\lambda A_\lambda v s\cos\beta=0, \tag{6b}$$
$$\frac{\partial V}{\partial S} = \lambda^2 s v^2+2\kappa^2 s^3-\lambda\kappa v^2 s\sin 2\beta+m_S^2 s-\frac{1}{2}\lambda A_\lambda v^2\sin 2\beta+\kappa A_\kappa s^2=0, \tag{6c}$$

where $v=\sqrt{v_1^2+v_2^2}$ and $\tan\beta=v_2/v_1$.

Here, let us classify the solutions of the stationary conditions of Eq. (6). It is important to emphasize here that, without very special relations among the parameters, when either two of v_1, v_2 and s are nonvanishing, the other must also be non-vanishing. This fact originates from the trilinear terms $\lambda A_\lambda H_1^0 H_2^0 S$ in the soft SUSY breaking terms and the quartic term $\lambda\kappa H_1^0H_2^0(S^*)^2$ in the F-term potential. Suppose that v_1 and v_2 are non-vanishing. Then, Eq. (6c) cannot be satisfied for a nonvanishing A_λ unless $S\neq 0$. A similar discussion is applicable to other cases. When we start with any combination of two non-vanishing vevs, we obtain the same result, that is, all three vevs should be non-vanishing. On the other hand, we find another type of solution, in which only one of v_1, v_2 and s is non-vanishing, while the others are vanishing. Therefore, a non-trivial solution of Eq. (6) is as follows: either three Higgs fields are non-vanishing or one Higgs field is non-vanishing. This observation justifies our strategy of analyses for unrealistic minima of the Higgs potential in the next section.

It is useful to express the soft SUSY breaking masses in terms of other parameters by rewriting the stationary conditions in Eq. (6) as follows:

$$m_{H_1}^2 = -\mu^2 - \frac{2\lambda^2}{g^2} m_Z^2 \sin^2\beta - \frac{1}{2} m_Z^2 \cos 2\beta + \mu\left(\frac{\kappa}{\lambda}\mu + A_\lambda\right)\tan\beta, \tag{7a}$$

$$m_{H_2}^2 = -\mu^2 - \frac{2\lambda^2}{g^2} m_Z^2 \cos^2\beta + \frac{1}{2} m_Z^2 \cos 2\beta + \mu\left(\frac{\kappa}{\lambda}\mu + A_\lambda\right)\cot\beta, \tag{7b}$$

$$m_S^2 = -\frac{2\lambda^2}{g^2} m_Z^2 - \frac{2\kappa^2}{\lambda^2}\mu^2 + \frac{2\lambda\kappa}{g^2} m_Z^2 \sin 2\beta + \frac{\lambda^2}{g^2}\frac{A_\lambda m_Z^2}{\mu}\sin 2\beta - \frac{\kappa}{\lambda} A_\kappa \mu, \tag{7c}$$

where $m_Z^2 = \frac{1}{2} g^2 v^2$ and $\mu = \lambda s$. Thus, given m_Z, we can use the parameters

$$\lambda, \quad \kappa, \quad A_\lambda, \quad A_\kappa, \quad \tan\beta \quad \text{and} \quad \mu, \tag{8}$$

instead of those in Eq. (4). Using these parameters, the realistic minimum of the potential, which reproduces the observed Z boson mass, can be written as

$$V_{\min} = -\lambda^2 \frac{m_Z^4 \sin^2 2\beta}{g^4} - \frac{m_Z^4 \cos^2 2\beta}{2g^2} + \overline{V}_{\min}^S, \tag{9}$$

where $\overline{V}_{\min}^S$ is the potential involving only s or μ/λ,

$$\overline{V}_{\min}^S = \frac{\kappa^2}{\lambda^4}\mu^4 + \frac{2}{3}\frac{\kappa}{\lambda^3} A_\kappa \mu^3 + \frac{1}{\lambda^2} m_S^2 \mu^2, \tag{10}$$

with m_S^2 given by Eq. (7c). In the following sections, we study unrealistic and/or CCB vacua and compare their depths with using Eq. (9).

If the vev of s (μ/λ) is sufficiently larger than the other vevs and the soft SUSY breaking parameters and the potential $\overline{V}_{\min}^S$ is dominant in the full potential, the typical depth of the realistic minimum can be estimated as

$$V_{\min} \simeq \overline{V}_{\min}^S \simeq -\frac{\kappa^2}{\lambda^4}\mu^4 - \frac{\kappa}{3\lambda^3} A_\kappa \mu^3. \tag{11}$$

Such an approximation is useful for estimating constraints, which will be shown in the next section.

Before we move on to the analysis of the scalar potential, we show the mass-squared matrices of the Higgs bosons in order to examine tachyonic masses in the next section. The number of degrees of freedom of the Higgs bosons is ten, three of which are absorbed by gauge bosons via the Higgs mechanism. The remaining seven physical degrees of freedom correspond to three CP-even Higgs bosons, two

CP-odd Higgs bosons and one charged Higgs boson. The mass-squared matrix of the CP-even Higgs bosons is real-symmetric and given by

$$M^2_{h,11} = m_Z^2 \cos^2\beta + \mu\left(\frac{\kappa}{\lambda}\mu + A_\lambda\right)\tan\beta, \tag{12a}$$

$$M^2_{h,22} = m_Z^2 \sin^2\beta + \mu\left(\frac{\kappa}{\lambda}\mu + A_\lambda\right)\cot\beta, \tag{12b}$$

$$M^2_{h,33} = \frac{4\kappa^2}{\lambda^2}\mu^2 + \frac{\kappa}{\lambda}A_\kappa\mu + \frac{\lambda^2}{g^2}\frac{A_\lambda m_Z^2}{\mu}\sin 2\beta, \tag{12c}$$

$$M^2_{h,12} = 2\left(\frac{\lambda^2}{g^2} - \frac{1}{4}\right)m_Z^2 \sin 2\beta - \mu\left(\frac{\kappa}{\lambda}\mu + A_\lambda\right), \tag{12d}$$

$$M^2_{h,13} = \frac{2\sqrt{2}\lambda}{g}\mu m_Z \cos\beta - \frac{\sqrt{2}\lambda}{g}m_Z\left(A_\lambda + \frac{2\kappa}{\lambda}\mu\right)\sin\beta, \tag{12e}$$

$$M^2_{h,23} = \frac{2\sqrt{2}\lambda}{g}\mu m_Z \sin\beta - \frac{\sqrt{2}\lambda}{g}m_Z\left(A_\lambda + \frac{2\kappa}{\lambda}\mu\right)\cos\beta. \tag{12f}$$

The mass-squared matrix of the CP-odd Higgs bosons is also real-symmetric and given by

$$M^2_{A,11} = \frac{2\mu}{\sin 2\beta}\left(A_\lambda + \frac{\kappa}{\lambda}\mu\right), \tag{13a}$$

$$M^2_{A,22} = \frac{\lambda^2}{g^2}m_Z^2\left(\frac{A_\lambda}{\mu} + \frac{4\kappa}{\lambda}\right)\sin 2\beta - \frac{3\kappa}{\lambda}A_\kappa\mu, \tag{13b}$$

$$M^2_{A,12} = \frac{\sqrt{2}\lambda}{g}m_Z\left(A_\lambda - \frac{2\kappa}{\lambda}\mu\right). \tag{13c}$$

It can be understood from Eqs. (12) and (13) that physical masses become tachyonic if λ is large, and hence the off-diagonal elements become comparable to or larger than the diagonal ones. The mass squared of the charged Higgs boson is

$$m^2_{H^\pm} = m_W^2 - \frac{2\lambda^2}{g^2}m_Z^2 + \frac{2\mu}{\sin 2\beta}\left(A_\lambda + \frac{\kappa}{\lambda}\mu\right), \tag{14}$$

where $m_W^2 = \frac{1}{2}g_2^2 v^2$ is the mass squared of the W boson. The charged Higgs boson mass squared can also be tachyonic when λ is sufficiently large. These mass-squared matrices are used in numerical calculations to find tachyonic mass regions.

§3. Constraints from unrealistic and Colour and/or Charge Breaking minima

In this section, we show that unrealistic minima and/or CCB minima appear in the scalar potential and derive necessary conditions to avoid these minima. First, we consider directions in which the neutral Higgs fields are non-vanishing while all other scalar fields are vanishing. Next, we consider directions in which squarks and/or sleptons as well as Higgs fields are non-vanishing. In the following, we discuss directions involving only the neutral Higgs fields and denote $H^0_{1,2}$ as $H_{1,2}$ for simplicity. As discussed in the previous section, when two of the Higgs fields develop their vevs, the other must develop its vev to satisfy the stationary conditions. Thus, analyses of the scalar potential are constrained to cases of either one or three non-vanishing Higgs fields. The realistic minimum given in the previous section is included along the direction, in which all three Higgs fields develop their vevs. Such a direction with all three non-vanishing Higgs vevs may include other unrealistic minima. Indeed, one unrealistic minimum with $|H_1| = |H_2| \neq 0$ and $S \neq 0$ will be studied below. However, analyses with three non-vanishing Higgs fields are so complicated in general that the potential minimum cannot be solved analytically. Hence, we restrict our discussions to four possible cases in which three Higgs fields are aligned as $|H_1| = |H_2| \neq 0$ and $S \neq 0$ so that the D-term and F_S-term are vanishing, and one of the three Higgs fields is non-vanishing. In fact, minima deeper than the realistic minimum are easily found along these directions. Such directions should be avoided to stabilize the realistic minimum. One of the main purposes of this paper is to show that these directions can be dangerous for the realization of a realistic minimum. Furthermore, along the directions with non-vanishing vevs of squarks and/or sleptons, we study CCB directions and derive necessary conditions to avoid these CCB minima according to general properties for CCB directions discussed in Ref. 47).

3.1. *Unrealistic minimum along* $|H_1| = |H_2| \neq 0$ *and* $S \neq 0$ *direction*

We consider the direction in which

$$|H_1| = |H_2| \neq 0, \quad S \neq 0, \tag{15}$$

where the up-type Higgs and down-type Higgs fields have the same vev. This direction corresponds to the so-called MSSM UFB-1 direction with a non-vanishing gauge singlet S. Along this direction, the D-term vanishes. Then, this would lead to a UFB direction in the MSSM without S. However, in the present case with $S \neq 0$, the potential is lifted up at a large value of the gauge singlet scalar; thus, an unrealistic minimum appears. The scalar potential along this direction is given by

$$\begin{aligned} V^{H_1H_2S} = {} & 2\lambda^2|S|^2|H_2|^2 + |F_S|^2 - \left(\lambda A_\lambda S H_1 H_2 - \frac{1}{3}\kappa A_\kappa S^3 + \text{h.c.}\right) \\ & + (m_{H_1}^2 + m_{H_2}^2)|H_2|^2 + m_S^2|S|^2, \end{aligned} \tag{16}$$

where

$$F_S = -\lambda H_1 H_2 + \kappa S^2. \tag{17}$$

The deepest minimum can be found along the direction in which trilinear couplings are negative and the F_S-term is vanishing, that is

$$S^2 = \frac{\lambda}{\kappa} H_1 H_2. \tag{18}$$

Note that the parameter κ must be positive to satisfy this relation. Then, the potential is written as

$$V^{H_1H_2S} = \hat{F}|H_2|^4 - 2\hat{A}|H_2|^3 + \hat{m}^2|H_2|^2, \tag{19}$$

where

$$\hat{F} = \frac{2\lambda^3}{\kappa}, \tag{20a}$$

$$\hat{A} = \lambda\sqrt{\frac{\lambda}{\kappa}}\left|A_\lambda - \frac{1}{3}A_\kappa\right|, \tag{20b}$$

$$\hat{m}^2 = m_{H_1}^2 + m_{H_2}^2 + \frac{\lambda}{\kappa}m_S^2. \tag{20c}$$

The trilinear term $\hat{A}$ can always be taken to be positive using the sign of S. By minimizing the potential of Eq. (19) with respect to $|H_2|$, we obtain $|H_2|$ at an extremal as

$$|H_2|_{\rm ext} = \frac{3\hat{A}}{4\hat{F}}\left(1 + \sqrt{1 - \frac{8\hat{m}^2\hat{F}}{9\hat{A}^2}}\right), \tag{21}$$

where $\hat{m}^2 \leq \frac{9\hat{A}^2}{8\hat{F}}$ is required for $|H_2|_{\rm ext}$ to be real. Note that the solution with a negative sign in front of the square root corresponds to the maximum potential; hence, we do not consider it here. Then, the minimum potential is obtained by inserting Eq. (21) as

$$V_{\rm min}^{H_1H_2S} = -\frac{1}{2}|H_2|_{\rm ext}^2(\hat{A}|H_2|_{\rm ext} - \hat{m}^2). \tag{22}$$

To realize the realistic minimum, the following condition is required,

$$V_{\rm min}^{H_1H_2S} \geq V_{\rm min}. \tag{23}$$

In the next section, we numerically examine this condition. Let us intuitively consider the implications of this condition by using some approximation. The extremal value is roughly estimated as

$$|H_2|_{\rm ext} \simeq \frac{|A_\kappa - 3A_\lambda|}{8}\sqrt{\frac{\kappa}{\lambda^3}}, \tag{24}$$

and the depth of the minimum is

$$V_{\rm min}^{H_1H_2S} \simeq -\frac{27}{1024}\frac{\kappa}{\lambda^3}A_\lambda^4, \tag{25}$$

for $A_\lambda \gg A_\kappa$. The typical magnitude of the minimum is determined by A_λ^4, and the minimum becomes deeper as κ becomes larger and λ becomes smaller.

3.2. *Unrealistic minimum along $H_2 \neq 0$ direction*

We consider the direction in which only the up-type Higgs field is non-vanishing. In most cases, the up-type Higgs scalar has a tachyonic mass to achieve EWSB in the NMSSM. Therefore, there exists a minimum along which the up-type Higgs field develops a vev, while other Higgs fields do not. At this minimum, EWSB does not occur successfully because down-type fermions cannot have masses. The existence of this minimum was first studied in Ref. 54). Although this condition is quite important, as we will show in the next section, it has not always been taken into account in the literature. Therefore, we reanalyze the unrealistic minimum along this direction and derive a necessary condition for the exclusion of parameters.

The scalar potential involving only the up-type Higgs field is given by

$$V^{H_2} = m_{H_2}^2 |H_2|^2 + \frac{1}{8} g^2 |H_2|^4, \tag{26}$$

where $m_{H_2}^2$ is given by Eq. (7b). The extremal value of $|H_2|$ is obtained as

$$|H_2|_{\rm ext}^2 = -\frac{4 m_{H_2}^2}{g^2}, \tag{27}$$

and the minimum potential is given by

$$V_{\rm min}^{H_2} = -\frac{2(m_{H_2}^2)^2}{g^2}. \tag{28}$$

If the minimum potential in Eq. (28) is deeper than the realistic minimum, the realistic minimum will not be realized. Even if the realistic minimum is realized once, it is unstable and may decay into this unrealistic minimum. Such a situation must be avoided by requiring

$$V_{\rm min}^{H_2} \geq V_{\rm min}. \tag{29}$$

In the next section, we numerically examine the condition Eq. (29). Here, let us take a certain limit to reduce the number of free parameters appearing under the condition and to intuitively consider the implications of this condition. We may expect that $|m_{H_2}^2| \sim \mu^2 \gg m_Z^2$ in a typical parameter space. The condition for parameters not satisfying the inequality, i.e., Eq. (29), can be expressed in a simple form when $\mu = \lambda s \gg m_Z$. The region excluded by the inequality Eq. (29) is given by

$$\kappa_- < \kappa < \kappa_+, \tag{30}$$

where

$$\kappa_\pm = \frac{\lambda}{(g^2 - 2\lambda^2 \cot^2\beta)\mu} \times \Bigg[-\frac{1}{6} g^2 A_\kappa - 2\lambda^2 \mu' \cot\beta \pm g \sqrt{2\lambda^2 \mu' \left(\mu' + \frac{1}{3} A_\kappa \cot\beta \right) + \frac{1}{36} g^2 A_\kappa^2} \Bigg], \tag{31}$$

with $\mu' = \mu - A_\lambda \cot\beta$. Furthermore, when $\mu \gg A_\lambda,\ A_\kappa$ and $g \gg \lambda$, κ_+ reduces to $\sqrt{2}\lambda^2/g$. That is, the excluded region is approximately written as

$$|\kappa| < \frac{\sqrt{2}}{g} \lambda^2, \tag{32}$$

which implies that a region with a small κ and a large λ is not allowed. Alternatively, in the above limit, the depth of this minimum given by Eq. (28), can be roughly estimated as

$$V_{\min}^{H_2} \simeq -\frac{2}{g^2}\mu^4. \tag{33}$$

Then, comparing this with the realistic minimum given by Eq. (11), the region excluded by Eq. (29) can be written as Eq. (32).

We have studied the unrealistic vacuum, where only H_2 develops its vev. Similarly, we can study the unrealistic vacuum, where only the down-type Higgs field H_1 develops its vev, but the others, H_2 and S, have vanishing vevs. The same results are applicable to Eqs. (26) – (28) with the replacement of H_2 and $m_{H_2}^2$ by H_1 and $m_{H_1}^2$, respectively. That is, along this direction, the potential is written as

$$V^{H_1} = m_{H_1}^2|H_1|^2 + \frac{1}{8}g^2|H_1|^4, \tag{34}$$

and the extremal value of H_1 and the corresponding potential minimum are obtained as

$$|H_1|_{\rm ext}^2 = -\frac{4m_{H_1}^2}{g^2}, \qquad V_{\min}^{H_1} = -\frac{2(m_{H_1}^2)^2}{g^2}, \tag{35}$$

as in Eqs. (27) and (28). The condition for avoiding this minimum is

$$V_{\min}^{H_1} > V_{\min}. \tag{36}$$

When $m_{H_1}^2$ is positive at the EWSB scale, such a minimum cannot be realized. Even if $m_{H_1}^2$ is negative but $m_{H_1}^2 > m_{H_2}^2$, this implies that $V_{\min}^{H_1} > V_{\min}^{H_2}$. In this case, the unrealistic minimum with $H_2 \neq 0$ is deeper and more important than that with $H_1 \neq 0$.

3.3. *Unrealistic minimum along $S \neq 0$ direction*

We consider the direction along which only S develops its vev. Along this direction, the sign of the trilinear term of S can be taken as negative and therefore a minimum always exists. This minimum can be deeper than that of the realistic minimum.

The scalar potential along this direction is given by

$$V^S(S) = \kappa^2|S|^4 - \frac{2}{3}|\kappa||A_\kappa||S|^3 + m_S^2|S|^2, \tag{37}$$

where m_S^2 is given by Eq. (7c). Minimizing the potential, we obtain the extremal value of S as

$$|S|_{\rm ext} = \frac{|A_\kappa|}{4|\kappa|}\left(1 + \sqrt{1 - 8\frac{m_S^2}{A_\kappa^2}}\right), \tag{38}$$

where $m_S^2 \leq \frac{1}{8}A_\kappa^2$ should be satisfied. Inserting Eq. (38) into Eq. (37), the minimum is given by

$$V_{\rm min}^S = -\frac{1}{6}|S|_{\rm ext}^2 \left(|\kappa||A_\kappa||S|_{\rm ext} - 3m_S^2\right). \tag{39}$$

A necessary condition to avoid this minimum is

$$V_{\rm min}^S \geq V_{\rm min}. \tag{40}$$

In the next section, we numerically examine the condition Eq. (40). Here, let us intuitively consider the implications of this condition by performing some approximation. The depth of the minimum is roughly estimated as

$$V_{\rm min}^S \simeq -\frac{A_\kappa^4}{384\kappa^2}. \tag{41}$$

Comparing this minimum with Eq. (11), one can see that Eq. (41) can be deeper than the realistic minimum if

$$|\kappa| \leq \frac{2}{5}\frac{|A_\kappa|}{|\mu|}\lambda. \tag{42}$$

In the next section, we show that the conditions Eqs. (29) and (40), as well as the requirement for no tachyonic masses, exclude a large region of the parameter space.

3.4. *Other unrealistic and charge and/or colour breaking minima*

Finally, we present constraints from other unrealistic and CCB directions in which not only squarks and/or sleptons but also the singlet scalar S are non-vanishing. The directions we consider here are the same directions studied in the MSSM but are different by a non-vanishing singlet scalar. In the MSSM, the CCB directions as well as UFB directions have been systematically studied in Refs. 7),8), 40)–46) and the general properties of these directions are summarized in Ref. 47). One of the general properties of the CCB and UFB directions is that the D-terms, which are positive quartic terms, must be vanishing or kept under control. This property is particularly important when the Yukawa couplings under consideration are smaller than the gauge coupling constants. In fact, the deepest CCB minima are found along vanishing D-term directions in the MSSM. Since the difference in the particle content of the NMSSM from that of the MSSM is the gauge singlet, the vanishing D-term directions are the same as those in the MSSM. Furthermore, when we consider the CCB and UFB directions of the MSSM with a vanishing singlet, $S = 0$, most of the constraints to avoid such directions are obtained from those in the MSSM by setting $\mu = 0$. Hence, nontrivial constraints are obtained along the direction in which the singlet scalar is non-vanishing, $S \neq 0$. For this purpose, it is sufficient to consider the CCB and UFB directions of the MSSM with the singlet scalar. Indeed, the MSSM scalar potential has three UFB directions:[47)]

$$\text{UFB}-1: \qquad |H_1| = |H_2| \neq 0, \tag{43a}$$

$$\text{UFB}-2: \qquad H_1,\ H_2,\ \tilde{L} \neq 0, \tag{43b}$$

$$\text{UFB}-3: \qquad H_2,\ \tilde{L},\ \tilde{Q},\ \tilde{d}_R \neq 0, \quad \tilde{d}_L = \tilde{d}_R \equiv \tilde{d}, \tag{43c}$$

where $\tilde{Q}$ and $\tilde{L}$ are chosen along $\tilde{d}_L$ and $\tilde{\nu}_L$, respectively. Thus, we study each direction while adding a non-vanishing gauge singlet S, except for the UFB-1 direction, which has already been studied in §3.1. Similar to 3.1, the potential is lifted up along these directions owing to the presence of S and an realistic minimum appears. In addition, we study a typical CCB direction of the MSSM while adding a non-vanishing gauge singlet. In the following, we only present results along these directions. Details of the calculations are found in Appendix B.

The first direction is that with the gauge singlet and the so-called MSSM UFB-2;

$$S,\ H_1,\ H_2,\ \tilde{L} \neq 0, \tag{44}$$

where $\tilde{L}$ is taken such that a sneutrino is non-vanishing. A necessary condition is obtained by requiring that the minimum is positive, i.e.,

$$\left(A_\lambda - \frac{1}{3}A_\kappa\right)^2 \leq (1+\gamma^2) \times \left[m_{H_1}^2 - m_{\tilde{L}}^2 + m_S^2 \frac{\lambda}{\kappa}\frac{1}{\gamma} + (m_{H_2}^2 + m_{\tilde{L}}^2)\frac{1}{\gamma^2}\right], \tag{45}$$

where γ is a real-positive parameter and smaller than 1. The most stringent constraint is obtained by minimizing the right-hand side. Then, the equation for the extremal value of γ is given as

$$2(m_{H_1}^2 - m_{\tilde{L}}^2)\gamma_{\text{ext}}^4 + m_S^2 \frac{\lambda}{\kappa}\gamma_{\text{ext}}(\gamma_{\text{ext}}^2 - 1) - 2(m_{H_2}^2 + m_{\tilde{L}}^2) = 0. \tag{46}$$

The second direction corresponds to the so-called MSSM UFB-3 direction with a non-vanishing gauge singlet, i.e.,

$$S,\ H_2,\ \tilde{L},\ \tilde{Q},\ \tilde{d}_R \neq 0, \quad \tilde{d}_L = \tilde{d}_R \equiv \tilde{d}, \tag{47}$$

where $\tilde{Q}$ and $\tilde{L}$ are chosen along $\tilde{d}_L$ and $\tilde{\nu}_L$, respectively. The vevs of $\tilde{d}_L$ and $\tilde{d}_R$ are chosen so that the F-term of H_1 vanishes. Then, following the calculations in (B·2), we find the constraint

$$|A_\kappa|^2 \leq 9\left[\frac{(m_{\tilde{Q}}^2 + m_{\tilde{d}_R}^2 + m_{\tilde{L}}^2)^2}{4(m_{H_2}^2 + m_{\tilde{L}}^2)}\frac{|\lambda|^2}{|Y_d|^2} - 2(m_{H_2}^2 + m_{\tilde{L}}^2) + m_S^2\right]. \tag{48}$$

The last direction we present is the so-called CCB-1 direction with the gauge singlet

$$S,\ H_2,\ \tilde{Q},\ \tilde{u}_R,\ \tilde{L} \neq 0, \tag{49}$$

and a necessary condition obtained from this direction is

$$\left(\alpha^2|A_u||Y_u| + \frac{1}{3}\sigma^3|\kappa||A_\kappa|\right)^2 \leq \left[\sigma^2(|\lambda|^2 + \sigma^2|\kappa|^2) + |Y_u|^2\alpha^2(\alpha^2+2)\right] \times \left[m_{H_2}^2 + \alpha^2(m_{\tilde{Q}}^2 + m_{\tilde{u}_R}^2) + \sigma^2 m_S^2 + (1-\alpha^2)\hat{m}_{\tilde{L}}^2\right], \tag{50}$$

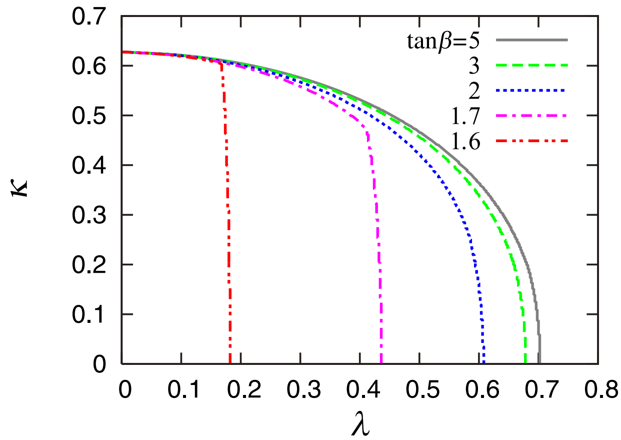

Fig. 1. (color online) Region excluded by the occurrence of a Landau pole on the λ-κ plane. Solid (gray), dashed (green), dotted (blue), dashed-dotted (violet) and dashed-dotted-dotted (red) curves correspond to $\tan\beta = 5,\ 3,\ 2,\ 1.7$ and 1.6, respectively. The region outside each curve is excluded.

where α and σ are real positive numbers and $0 \leq \alpha \leq 1$. The most stringent constraint is obtained by minimizing Eq. (50) with respect to α and σ, which can be performed numerically. Similarly, we can analyze other MSSM CCB directions while taking $S \neq 0$. At any rate, the constraints Eqs. (45), (48) and (50) include more parameters such as $m^2_{\tilde{L}}$ and $m^2_{\tilde{Q}}$. Thus, we focus on analyzing numerically analyzing the constraints of §§3.1 – 3.3 in the next section.

§4. Numerical analysis

We present numerical results of the constraints obtained from the unrealistic minima $V^{H_1H_2S}_{\rm min} \geq V_{\rm min}$ Eq. (23), $V^{H_2}_{\rm min} \geq V_{\rm min}$ Eq. (29) and $V^{S}_{\rm min} \geq V_{\rm min}$ Eq. (40) discussed in the previous section. In addition to these constraints, we also take into account the conditions that (i) the physical masses of the neutral and charged Higgs scalars are nontachyonic, and (ii) the parameter, λ and κ, have no Landau poles up to the GUT scale (1.6×10^{16} GeV). For condition (ii), we solve the renormalization group (RG) equations at one loop[8),55)] from the EWSB scale to the GUT scale and require that λ and $|\kappa|$ are smaller than 2π at the GUT scale.[11),56)] Note that in the table and figures shown in this section, the values of parameters are given at the EWSB scale.

Figure 1 shows the region excluded by the occurrence of a Landau pole on the λ-κ plane. Here, we used the running top quark mass, $m_t = 165$ GeV as the input. Solid (gray), dashed (green), dotted (blue), dashed-dotted (violet) and dashed-dotted-dotted (red) curves correspond to $\tan\beta = 5,\ 3,\ 2,\ 1.7$ and 1.6, respectively. The region outside each curve is excluded. One can see that λ is more constrained when $\tan\beta$ is small, on the other hand, the upper bound on κ remains constant at approximately 0.63. This is because the RG evolution of λ is directly related to the top Yukawa coupling. When $\tan\beta$ is small, the top Yukawa coupling at a low energy

Table I. Reference points for numerical analysis taken from Refs. 37) and 39).

point	$\tan\beta$	A_λ (GeV)	A_κ (GeV)	$\mu = \lambda s$ (GeV)
1	3	−200	−50	110
2	3	200	−200	110
3	3	50	−50	110
4	5	450	50	200

is large and it grows quickly as the energy scale increases. Then, λ is driven to a large value as the top Yukawa coupling grows. On the other hand, the RG evolution of κ is proportional to κ^2 and depends on the top Yukawa coupling only through λ. Therefore, κ starts to grow after the top Yukawa coupling and λ become sufficiently larger than 2π. As we can see in Fig. 1, the maximum λ becomes much smaller for $\tan\beta < 2$ and it disappears when $\tan\beta \leq 1.5$. In the following, we choose moderate values of $\tan\beta$ to analyze the constraints obtained from the unrealistic minima.

We use the parameter sets discussed in Refs. 37) and 39) as illustrated examples. In Table I, we list four reference points taken from 37) and 39) which lead to light spectra of Higgs scalars. Such a light Higgs scalar is characteristic of the NMSSM, which is utilized for sneutrino dark matter.[57),58)] In fact, as we will see, the conditions Eqs. (23), (29) and (40) exclude larger regions on the λ-κ plane.

Figure 2 shows regions excluded by $V_{\rm min}^{H_1H_2S} > V_{\rm min}$ (a), $V_{\rm min} > V_{\rm min}^{H_2}$ (b) and $V_{\rm min} > V_{\rm min}^{S}$ (c) as well as the tachyonic Higgs masses (d) on the λ-κ plane. In panel (e), all conditions in addition to the Landau pole condition are superposed. In panel (a), we can see that the condition $V_{\rm min}^{H_1H_2S} > V_{\rm min}$ excludes a wider region for a large λ. One may consider that this minimum can be a realistic minimum because three Higgs fields develop vevs. However, as indicated in Fig. 1, no region is allowed for $\tan\beta = 1$ with the occurrence of a Landau pole. The reason why a region of large λ is excluded is as follows. From Eq. (25), $V_{\rm min}^{H_1H_2S}$ becomes shallower as λ becomes larger and its depth is typically determined by A_λ^4. However, the realistic minimum has a similar dependence, and its depth is determined by $A_\kappa\mu^3$, as shown in Eq. (11). Therefore, $V_{\rm min}^{H_1H_2S}$ becomes deeper than the realistic minimum for $|A_\lambda| > A_\kappa,\ \mu$. Furthermore, (20c) is negative in a wide region of parameter space when A_λ is negative, and the minimum, $V_{\rm min}^{H_1H_2S}$ (22), appears in this region. Thus, this condition can exclude a large region of the parameter space when A_λ is large and negative.

Panel (b) shows that the condition $V_{\rm min}^{H_2} > V_{\rm min}$ also excludes a wider region for a large λ. This can be understood as follows: Recall from (28) and (7b) that $V_{\rm min}^{H_2} \propto -(m_{H_2}^2)^2$ and $|m_{H_2}^2| \sim \lambda^2 m_Z^2$. Therefore $V_{\rm min}^{H_2}$ becomes deeper as λ increases. On the other hand, from (11), $V_{\rm min} \simeq \overline{V}_{\rm min}^S$ is a polynomial of μ/λ. For a fixed μ, $|\overline{V}_{\rm min}^S|$ decreases as λ increases. Hence, the minimum $\overline{V}_{\rm min}^S$, as well as $V_{\rm min}$, becomes shallower as λ increases. In addition, the λ-independent term of $V_{\rm min}^{H_2}$ is $-\mu^4/(g_1^2+g_2^2)$, while that of $\overline{V}_{\rm min}^S$ appears in $m_S^2 s^2$, i.e. , $A_\lambda \mu m_Z^2/(g_1^2+g_2^2)\sin 2\beta$. It is expected that $-\mu^4/(g_1^2+g_2^2) < A_\lambda \mu m_Z^2/(g_1^2+g_2^2)\sin 2\beta$. Thus, $V_{\rm min}^{H_2}$ is deeper than $V_{\rm min}$ for a large λ. This result can be seen more easily in (31). When λ is large,

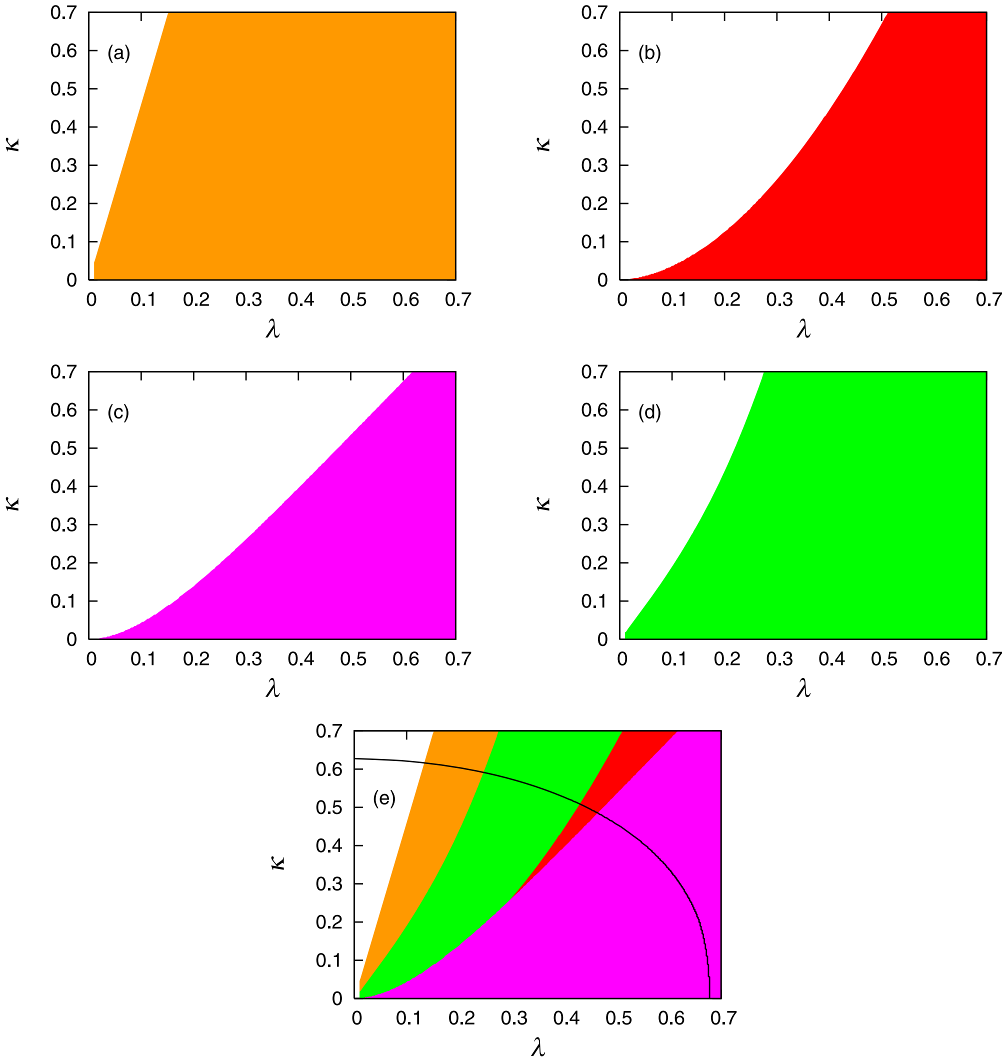

Fig. 2. (color online) Excluded region for point 1. Regions (coloured regions) with $V_{\rm min}^{H_1H_2S} > V_{\rm min}$, $V_{\rm min}^{H_2} > V_{\rm min}$ and $V_{\rm min}^{S} > V_{\rm min}$ are shown in (a), (b) and (c), respectively, and that with tachyonic Higgs masses is shown in (d). All conditions with the Landau pole condition (black curve) are superposed in panel (e). The region excluded by the Landau pole is outside of the curve.

the approximate condition κ_+ becomes

$$\kappa_+ \simeq \frac{\lambda^2}{g^2\mu}(\sqrt{2}g|\mu'| - 2\lambda\mu' \cot\beta), \tag{51}$$

where we used $\mu' \gg g^2 A_\kappa$.

In panel (c), the region excluded by $V_{\rm min}^S > V_{\rm min}$ is shown. It is seen that this condition also excludes a larger region for a large λ. The reason for this is almost the same as that for panel (b). $|\overline{V}_{\rm min}^S|$ in $V_{\rm min}$ decreases as λ increases. On the other hand, the λ dependence of $V_{\rm min}^{S}$ appears through m_S^2, which also decreases as λ increases. A smaller m_S^2 leads to a higher $|V_{\rm min}^{S}|$. Thus, the region with a large λ is excluded by the constraint $V_{\rm min}^{S} > V_{\rm min}$.

The region excluded by tachyonic Higgs masses is shown in panel (d). In this region, minima deeper than the realistic one exist and hence the EWSB vacuum is unstable. Such minima can be $V_{\rm min}^{H_1H_2S}$, $V_{\rm min}^{H_2}$ and $V_{\rm min}^{S}$. The tachyonic masses are simply due to large off-diagonal elements in the mass matrices. From the mass matrices given by Eqs. (12) and (13), one can understand that the off-diagonal elements become larger than or comparable to the diagonal elements when λ is large. A large λ leads to tachyonic masses after the diagonalization of the mass matrices. Thus, again, a large λ is excluded.

In the end, in panel (e), we superpose all constraints with that for avoiding the occurrence of Landau poles. The region excluded by Landau poles of λ, κ and the top Yukawa coupling is indicated outside the solid (black) curve. One can see that a large λ is excluded by unphysical minima and tachyonic masses, while a large κ is excluded by the Landau pole condition. One can also see that the condition $V_{\rm min}^{H_1H_2S} > V_{\rm min}$ is a tighter constraint than that from the tachyonic condition. This means that even if the EWSB vacuum has no tachyonic directions, a deeper minimum along the $H_1 = H_2 \neq 0$ and $F_S = 0$ direction exists and makes the EWSB vacuum unstable. Therefore, it is important to take this constraint into account for the analysis. Finally, it is worthwhile mentioning that the region allowed for this point is located within $\lambda \leq 0.15$ and $\kappa \leq 0.62$.

Figure 3 shows the excluded region for point 2. Each panel corresponds to the same constraints of the unrealistic minima as in Fig. 2. In panel (a), we see that the condition $V_{\rm min}^{H_1H_2S} > V_{\rm min}$ is not as tight as that for point 1. As explained for Fig. 2, $\hat{m}^2$ in (20c) is positive in a large region of the parameter space for a positive A_λ, and hence $V_{\rm min}^{H_1H_2S}$ does not appear. In panel (c), we also see that the region excluded by $V_{\rm min}^{S} > V_{\rm min}$ is weaker than that for point 1. This is because m_S^2 is positive and larger than $\frac{1}{8}A_\kappa^2$ in a wide region of the parameter space, and hence $V_{\rm min}^{S}$ does not appear. Panel (d) shows all constraints with those for avoiding the occurrence of Landau poles. In addition, the blue region corresponds to the region where $V_{\rm min}$ is positive. We can see that the condition $V_{\rm min}^{H_2} > V_{\rm min}$ is a tighter constraint than that from the tachyonic condition. This means that a deeper minimum appears along the $H_2 \neq 0$ direction and that EWSB vacuum is unstable. Therefore, the constraint Eq. (29) is also important for the analysis. Again, the region allowed for this point is located within $\lambda \leq 0.5$ and $\kappa \leq 0.62$.

In Fig. 4, the same insets in Fig. 2(e) are shown for points 3 and 4. In panel (a), it is seen that the difference from point 2 is that a wider region for a large λ is excluded by the conditions of the unrealistic minima and the tachyonic masses. This result is non-trivial and is due to the complicated dependences on the parameters. The trilinear couplings A_λ and A_κ for point 3 are smaller than those for point 2. The smaller couplings result in shallow depths of not only the unrealistic minima but also the realistic minimum. The realistic minimum tends to be shallower than the unrealistic ones for smaller trilinear couplings. In panel (b), a region of negative κ values is largely excluded because A_κ is negative. It is seen that a wide region of

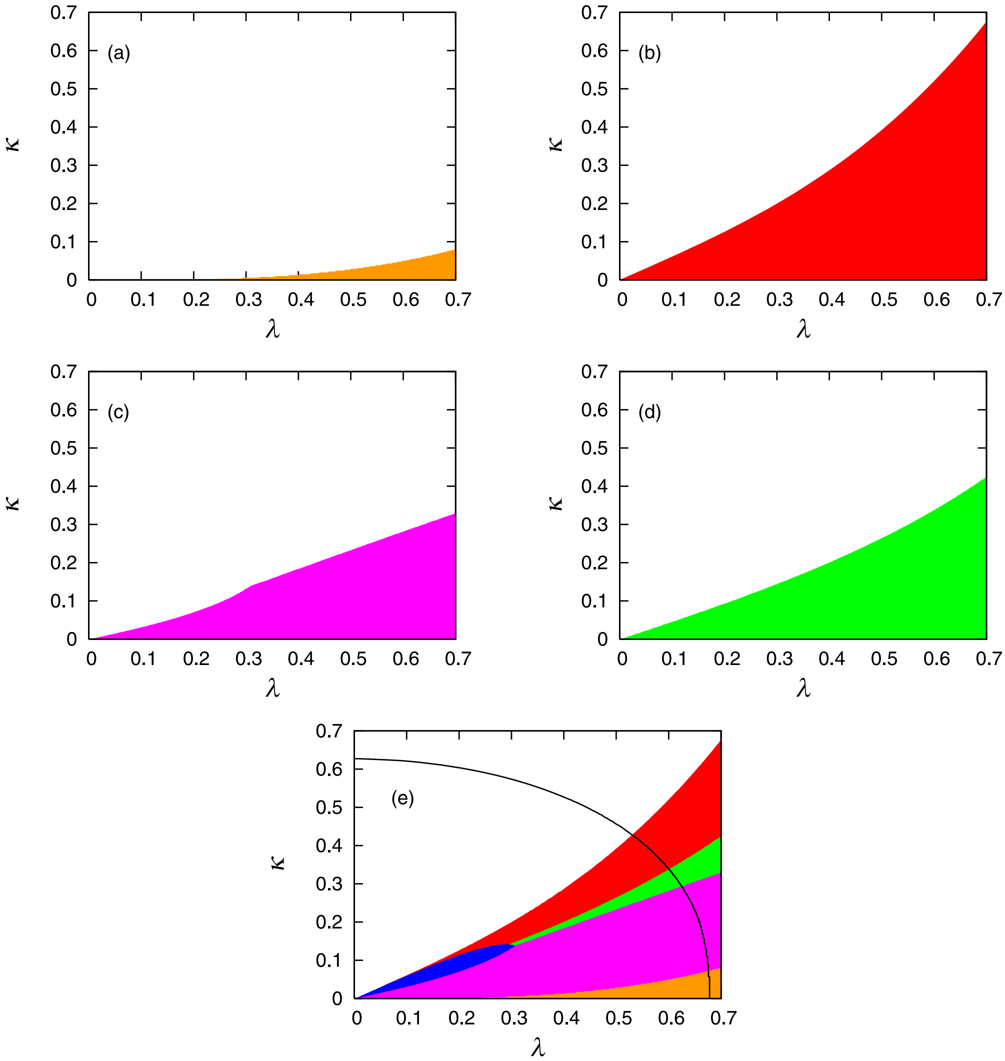

Fig. 3. (color online) Excluded region for point 2. Each panel is the same as for point 1. In panel (e), the blue region indicates the excluded region where $V_{\rm min}$ is positive.

large λ is excluded by the condition $V^S_{\rm min} > V_{\rm min}$, and that for small λ values it is excluded by the condition from tachyonic masses. Thus, the condition $V^S_{\rm min} > V_{\rm min}$ is also important.

§5. Conclusion and discussion

In this paper, we have analyzed the scalar potential of the NMSSM at the tree level and studied constraints from unphysical minima on which the EWSB does not occur successfully and CCB minima on which colour and/or electric charge symmetry is broken.

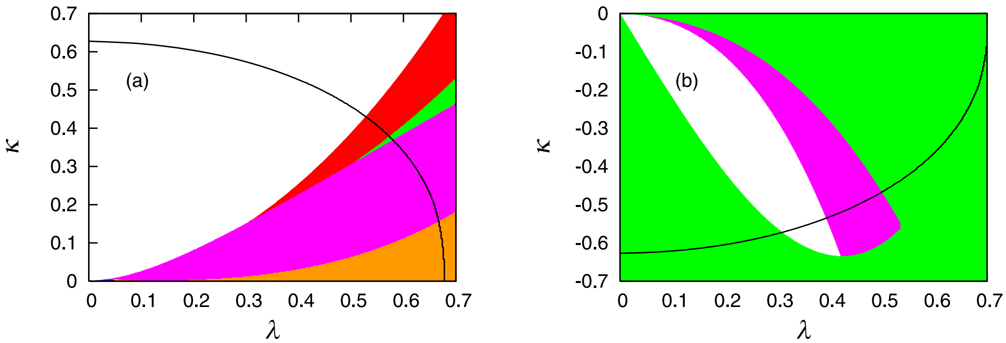

Fig. 4. (color online) Excluded regions for points 3 and 4. Panel (a) is for point 3 and panel (b) is for point 4. The colour indicates the same condition as that for the panels in Fig. 3.

In §3, we derived explicit expressions for unrealistic minima along which $H_1 = H_2 \neq 0$ with $F_S = 0$ and only one of the three Higgs fields develop its vevs. These unrealistic minima threaten the realization of EWSB if they are deeper than the EWSB vacuum. Indeed, using some approximations, we showed that such minima can be deeper than realistic minima for a large λ. Constraints from other directions involving squarks and sleptons were also derived.

In §4, we numerically studied the constraints to avoid unrealistic minima as well as the occurrence of Landau poles and tachyonic masses. Regarding the conditions for avoiding Landau poles, it was found in Fig. 1 that the parameter λ is significantly excluded for $\tan\beta < 2$ and that the allowed region disappears for $\tan\beta < 1.5$. Thus, the direction with $H_1 = H_2 \neq 0$ can never be a realistic minimum under the Landau pole condition. Then, we chose four points of the parameters with a moderate $\tan\beta$ as illustrated examples, which correspond to the light spectra of Higgs scalars. In Fig. 2, we showed that most of the region on the λ-κ plane is ruled out for point 1. The most stringent constraints for this point come from $H_1 = H_2 \neq 0$ with the $F_S = 0$ direction and the absence of Landau poles. This result is rather general for points with large negative A_λ because this unrealistic minimum widely appears for a negative A_λ and its depth is determined by A_λ^4. In Fig. 3, it was shown that the constraints from the H_2 direction and Landau poles exclude a wider region of large λ and κ in point 2. This is because $V_{\rm min}^{H_2}$ becomes deeper while $V_{\rm min}$ becomes shallower as λ increases. A similar result is shown in Fig. 4(a) for point 3. In Fig. 4(b), we also found that a large region of the parameter space is ruled out for a negative κ. Importantly, a large λ is generally excluded by the constraints. The stringent constraints are those from the S direction and the tachyonic masses. Our results imply that each of the constraints is significant. Since the constraints are independent of each other, it is important to apply all constraints considered here in the analyses of the NMSSM.

Finally, we discuss the implications of our results. The coupling constant λ is important for increasing the Higgs mass at the tree level. However, from our numerical analysis, we saw that a large λ is not allowed from the constraints. This implies that the SM-like Higgs mass should be similar to that of the MSSM at the tree level. Thus, our constraints should be important for the spectrum of the Higgs sector as well as in dark matter physics. One-loop corrections can give sizable contributions to the Higgs masses but may not change the structure of vacua drastically in the SUSY model. If the lifetime of vacua is longer than the age of the universe, a realistic vacuum becomes metastable and the parameter space is not constrained. The lifetime of vacua is proportional to $\exp(-B)$, where B is a Euclidean action for bounce solutions.[59)–61)] For the lifetime to be longer than the age of the universe, B is required to be larger than 400. We estimated the exponent B for the false vacuum shown in §3.1 using the methods in 62) and 63) and found that B is roughly on the order of $10 - 100$. Thus, our results should be still valid if the lifetime is taken into consideration. However, detailed studies of the lifetime and radiative corrections are important to exclude parameter regions. We will study these aspects in our future works.

Acknowledgements

T. K. is supported in part by a Grant-in-Aid for Scientific Research No. 20540266 and the Grant-in-Aid for the Global COE Program "The Next Generation of Physics, Spun from Universality and Emergence" from the Ministry of Education, Culture, Sports, Science and Technology of Japan. O. S. is supported in part by scientific research grants from Hokkai-Gakuen and thanks the Yukawa Institute for Theoretical Physics of Kyoto University, where this work was completed during the YITP-T-10-05 on "Cosmological Perturbation and Cosmic Microwave Background". T. S. is a Yukawa Fellow and his work is partially supported by the Yukawa Memorial Foundation, a Graint-in-Aid for Young Scientists (B) No. 23740190 and the Sasakawa Scientific Research Grant from The Japan Science Society. The work of Y. Kanehata and Y. Konishi is supported by the Maskawa Institute of Kyoto Sangyo University.

Appendix A
—— *Scalar Potential* ——

In this appendix, we give notations of the scalars and the scalar potential of the NMSSM. Throughout this article, flavour indices are suppressed for simplicity.

The down-type and up-type Higgs scalars are respectively denoted as

$$H_1 = \begin{pmatrix} H_1^1 \\ H_1^2 \end{pmatrix}, \quad H_2 = \begin{pmatrix} H_2^1 \\ H_2^2 \end{pmatrix}, \tag{A·1}$$

where H_1^1 and H_2^2 are electrically neutral components and H_1^2 (H_2^1) are negatively (positively) charged components. The gauge singlet scalar is denoted by S. The left-handed and right-handed squarks are denoted as

$$\tilde{Q} = \begin{pmatrix} \tilde{u}_L \\ \tilde{d}_L \end{pmatrix}, \quad \tilde{u}_R,\ \tilde{d}_R, \tag{A·2}$$

and those of sleptons are denoted as

$$\tilde{L} = \begin{pmatrix} \tilde{\nu}_L \\ \tilde{e}_L \end{pmatrix}, \quad \tilde{e}_R. \tag{A·3}$$

The superpotential of the NMSSM is given by

$$\mathcal{W}_{\rm NMSSM} = Y_d \hat{H}_1 \cdot \hat{Q} \hat{D}_R^c + Y_u \hat{H}_2 \cdot \hat{Q} \hat{U}_R^c + Y_e \hat{H}_1 \cdot \hat{L} \hat{E}_R^c - \lambda \hat{S} \hat{H}_1 \cdot \hat{H}_2 + \frac{1}{3} \kappa \hat{S}^3, \tag{A·4}$$

where a "hat" symbol denotes a superfield of each chiral multiplet and a "dot" symbol represents an inner product for $SU(2)$ doublets, $A \cdot B \equiv A^1 B^2 - A^2 B^1$. The Yukawa coupling constants for up-type quarks, down-type quarks and leptons are denoted by Y_u, Y_d and Y_e, respectively, and that for the singlet fermion is denoted by λ. The self-coupling constant of the singlet is κ. The scalar potential V is divided into three parts, which consist of F, D and the soft SUSY breaking terms:

$$V = V_F + V_D + V_{\rm soft}. \tag{A·5}$$

The F term potential V_F is given by the sum of the absolute squares of all the matter auxiliary fields;

$$V_F = \sum_{i={\rm matter}} |F_i|^2, \tag{A·6}$$

where

$$F^*_{H_1^1} = -\lambda s H_2^2 + Y_d \tilde{d}_L \tilde{d}^*_R + Y_e \tilde{e}_L \tilde{e}^*_R, \tag{A·7a}$$
$$F^*_{H_1^2} = \lambda s H_2^1 - Y_d \tilde{u}_L \tilde{d}^*_R - Y_e \tilde{\nu}_L \tilde{e}^*_R, \tag{A·7b}$$
$$F^*_{H_2^1} = \lambda s H_1^2 + Y_u \tilde{d}_L \tilde{u}^*_R, \tag{A·7c}$$
$$F^*_{H_2^2} = -\lambda s H_1^1 - Y_u \tilde{u}_L \tilde{u}^*_R, \tag{A·7d}$$
$$F^*_S = \lambda \left(H_1^1 H_2^2 - H_1^2 H_2^1 \right) - \kappa s^2, \tag{A·7e}$$
$$F^*_{\tilde{d}_L} = Y_d H_1^1 \tilde{d}^*_R + Y_u H_2^1 \tilde{u}^*_R, \tag{A·7f}$$
$$F^*_{\tilde{u}_L} = -Y_d H_1^2 \tilde{d}^*_R - Y_u H_2^2 \tilde{u}^*_R, \tag{A·7g}$$
$$F^*_{\tilde{e}_L} = Y_e H_1^1 \tilde{e}^*_R, \tag{A·7h}$$
$$F^*_{\tilde{\nu}_L} = -Y_e H_1^2 \tilde{e}^*_R, \tag{A·7i}$$
$$F_{\tilde{d}_R} = Y_d \left(H_1^1 \tilde{d}_L - H_1^2 \tilde{u}_L \right), \tag{A·7j}$$
$$F_{\tilde{u}_R} = Y_u \left(H_2^1 \tilde{d}_L - H_2^2 \tilde{u}_L \right), \tag{A·7k}$$
$$F_{\tilde{e}_R} = Y_e \left(H_1^1 \tilde{e}_L - H_1^2 \tilde{\nu}_L \right). \tag{A·7l}$$

The D term potential V_D is given by the sum of squares of all the gauge auxiliary fields;

$$V_D = \frac{1}{2} \Big((D^a_{SU(3)})^2 + (D^a_{SU(2)})^2 + (D_{U(1)})^2 \Big), \tag{A·8}$$

where the subscripts represent gauge groups and a runs from 1 to 8 (3) for $SU(3)$ ($SU(2)$). Summation over a should be understood. The auxiliary fields are given by

$$D^a_{SU(3)} = g_3 \left(\tilde{Q}^\dagger \frac{\lambda^a}{2} \tilde{Q} - \tilde{u}_R^* \frac{\lambda^a}{2} \tilde{u}_R - \tilde{d}_R^* \frac{\lambda^a}{2} \tilde{d}_R \right), \tag{A·9a}$$

$$D^a_{SU(2)} = g_2 \big(\tilde{Q}^\dagger T^a \tilde{Q} + \tilde{L}^\dagger T^a \tilde{L} + H_1^\dagger T^a H_1 + H_2^\dagger T^a H_2 \big), \tag{A·9b}$$

$$D_{U(1)} = g_1 \left(\frac{1}{6} \tilde{Q}^\dagger \tilde{Q} - \frac{2}{3} \tilde{u}_R^* \tilde{u}_R + \frac{1}{3} \tilde{d}_R^* \tilde{d}_R - \frac{1}{2} \tilde{L}^\dagger \tilde{L} + \tilde{e}_R^* \tilde{e}_R - \frac{1}{2} H_1^\dagger H_1 + \frac{1}{2} H_2^\dagger H_2 \right), \tag{A·9c}$$

where g_i $(i = 1, 2, 3)$ are gauge coupling constants, and λ^a and T^a are the Gell-Mann and Pauli matrices, respectively. The scalar potential $V_{\rm soft}$ with soft SUSY breaking terms is given as

$$\begin{aligned} V_{soft} = {} & m_{H_1}^2 H_1^\dagger H_1 + m_{H_2}^2 H_2^\dagger H_2 + m_S^2 S^\dagger S + \left(\frac{1}{3} \kappa A_\kappa S^3 - \lambda A_\lambda S H_1 \cdot H_2 + \text{h.c.} \right) \\ & + m_{\tilde{Q}}^2 \tilde{Q}^\dagger \tilde{Q} + m_{\tilde{u}_R}^2 \tilde{u}_R^* \tilde{u}_R + m_{\tilde{d}_R}^2 \tilde{d}_R^* \tilde{d}_R + m_{\tilde{L}}^2 \tilde{L}^\dagger \tilde{L} + m_{\tilde{e}_R}^2 \tilde{e}_R^* \tilde{e}_R \\ & + \big(A_d Y_d H_1 \cdot \tilde{Q} \tilde{d}_R^* + A_u Y_u H_2 \cdot \tilde{Q} \tilde{u}_R^* + A_e Y_e H_1 \cdot \tilde{L} \tilde{e}_R^* + \text{h.c.} \big), \end{aligned} \tag{A·10}$$

where A_λ and A_κ are trilinear couplings for Higgs fields and A_i $(i = u, d, e)$ are those for squarks and sleptons. The soft SUSY breaking masses squared are denoted by m_i^2 $(i = H_1, H_2, \tilde{Q}, \tilde{u}_R, \tilde{d}_R, \tilde{L}, \tilde{e}_R)$.

Appendix B
—— *Unrealistic Minima Involving Squarks and Sleptons* ——

In this appendix, we derive constraints to avoid the unrealistic minima discussed in §3.4. In the following, we respectively denote H_1^1 and H_2^2 as H_1 and H_2 for simplicity.

B.1. *MSSM UFB-2 direction with gauge singlet*

We analyze the so-called MSSM UFB-2 direction with the gauge singlet:

$$S,\ H_1,\ H_2,\ \tilde{L} \neq 0, \tag{B·1}$$

where $\tilde{L}$ is chosen along $\tilde{\nu}_L$. The scalar potential along this direction is

$$\begin{aligned} V_{\rm UFB-2} = {} & \lambda^2 |S|^2 (|H_1|^2 + |H_2|^2) + |F_S|^2 + m_{H_1}^2 |H_1|^2 + m_{H_2}^2 |H_2|^2 + m_{\tilde{L}}^2 |\tilde{\nu}_L|^2 + m_S^2 |S|^2 \\ & - 2\lambda A_\lambda H_1 H_2 S - \frac{2}{3} \kappa A_\kappa S^3 + \frac{1}{8} g^2 (|H_2|^2 - |H_1|^2 - |\tilde{\nu}_L|^2)^2, \end{aligned} \tag{B·2}$$

where F_S is given by (17). By minimizing $|\tilde{\nu}_L|$, we have

$$|\tilde{\nu}_L|^2 = - \left(4 \frac{m_{\tilde{L}}^2}{g^2} - |H_2|^2 + |H_1|^2 \right), \tag{B·3}$$

where $4m_{\tilde{L}}^2/g^2 - |H_2|^2 + |H_1|^2 < 0$ must be satisfied. Inserting this into the potential, the potential is given by

$$\begin{aligned} V_{\rm UFB-2} = &-2\frac{m_{\tilde{L}}^4}{g^2} + \lambda^2|S|^2(|H_1|^2+|H_2|^2) + |F_S|^2 \\ &+ (m_{H_1}^2 - m_{\tilde{L}}^2)|H_1|^2 + (m_{H_2}^2 + m_{\tilde{L}}^2)|H_2|^2 + m_S^2|S|^2 \\ &- 2\lambda A_\lambda S H_1 H_2 + \frac{2}{3}\kappa A_\kappa S^3. \end{aligned} \tag{B·4}$$

By choosing S so that F_S is vanishing as (18) and by parameterizing the vev as $|H_1| = \gamma|H_2|$, then the potential can be written in a form similar to (23),

$$V_{\rm UFB-2} = \hat{F}|H_2|^4 - 2\hat{A}|H_2|^3 + \hat{m}^2|H_2|^2 - 2\frac{m_{\tilde{L}}^4}{g^2}, \tag{B·5}$$

where

$$\hat{F} = \frac{\lambda^3}{\kappa}\gamma(1+\gamma^2), \tag{B·6a}$$

$$\hat{A} = \left(\left|A_\lambda - \frac{1}{3}A_\kappa\right|\right)\sqrt{\frac{\lambda^3}{\kappa}\gamma^3}, \tag{B·6b}$$

$$\hat{m}^2 = (m_{H_1}^2 - m_{\tilde{L}}^2)\gamma^2 + (m_{H_2}^2 + m_{\tilde{L}}^2) + m_S^2\frac{\lambda}{\kappa}\gamma. \tag{B·6c}$$

When the constant term in the potential is negligible, the extremal value of $|H_2|$ and the depth of the minimum are obtained by simply replacing $\hat{F}$, $\hat{A}$ and $\hat{m}^2$ in (21) and (22) with (B·6). The typical magnitudes of the extremal value and the depth of the minimum are similar to those in 3.1. To avoid the minimum, we obtain the constraint

$$\left(A_\lambda - \frac{1}{3}A_\kappa\right)^2 \le (1+\gamma^2) \times \left[m_{H_1}^2 - m_{\tilde{L}}^2 + m_S^2\frac{\lambda}{\kappa}\frac{1}{\gamma} + (m_{H_2}^2 + m_{\tilde{L}}^2)\frac{1}{\gamma^2}\right]. \tag{B·7}$$

Minimizing the right-hand side with respect to γ, we find that the extremal value of γ has to satisfy the relation

$$2(m_{H_1}^2 - m_{\tilde{L}}^2)\gamma_{\rm ext}^4 + m_S^2\frac{\lambda}{\kappa}\gamma_{\rm ext}(\gamma_{\rm ext}^2 - 1) - 2(m_{H_2}^2 + m_{\tilde{L}}^2) = 0. \tag{B·8}$$

B.2. *MSSM UFB-3 direction with gauge singlet*

Here, we study the so-called MSSM UFB-3 direction with the gauge singlet S. That is, the direction we analyze is

$$S,\ H_2,\ \tilde{L},\ \tilde{Q},\ \tilde{d}_R \neq 0, \quad \tilde{d}_L = \tilde{d}_R \equiv \tilde{d}, \tag{B·9}$$

where $\tilde{Q}$ and $\tilde{L}$ are chosen along $\tilde{d}_L$ and $\tilde{\nu}_L$, respectively. The vevs of $\tilde{d}_L$ and $\tilde{d}_R$ are chosen so that the F term of H_1 vanishes. Using the parametrization,

$$|\tilde{L}| = \gamma_L|H_2|, \quad |S| = \sigma|H_2|, \tag{B·10}$$

the condition for $F_{H_1} = 0$ is expressed as

$$\gamma_L^2 = 1 + \frac{\lambda}{|Y_d|}\sigma. \tag{B·11}$$

The scalar potential can be written in the same form as (23) with

$$\hat{F}(\sigma) = |\kappa|^2\sigma^4, \tag{B·12a}$$

$$\hat{A}(\sigma) = \frac{1}{3}|A_\kappa||\kappa|\sigma^3, \tag{B·12b}$$

$$\hat{m}^2(\sigma) = m_{H_2}^2 + m_S^2\sigma^2 + m_{\tilde{L}}^2 + (m_{\tilde{Q}}^2 + m_{\tilde{d}_R}^2 + m_{\tilde{L}}^2)\frac{\lambda}{|Y_d|}\sigma. \tag{B·12c}$$

By repeating the same procedure, the extremal value is obtained as

$$|H_2|_{\rm ext} = \frac{|A_\kappa|}{4\sigma|\kappa|} \times \left[1+\sqrt{1-\frac{8\left\{m_{H_2}^2+m_{\tilde{L}}^2+m_S^2\sigma^2 + \frac{\lambda\sigma}{|Y_d|}(m_{\tilde{Q}}^2+m_{\tilde{d}_R}^2+m_{\tilde{L}}^2)\right\}}{|A_\kappa|^2\sigma^2}}\,\right], \tag{B·13}$$

and the minimum of the potential is estimated roughly as

$$V_{\rm min} \sim -\frac{1}{384}\frac{|A_\kappa|^4}{|\kappa|^2}. \tag{B·14}$$

Thus, this minimum can be deeper than the realistic minimum if $|\kappa| \ll 1$. A necessary condition for avoiding this minimum is given by

$$|A_\kappa|^2 \le 9\left[(m_{\tilde{Q}}^2 + m_{\tilde{d}_R}^2 + m_{\tilde{L}}^2)\frac{\lambda}{|Y_d|}\frac{1}{\sigma} + (m_{H_2}^2 + m_{\tilde{L}}^2)\frac{1}{\sigma^2} + m_S^2\right]. \tag{B·15}$$

The stringent constraint is obtained by minimizing the right-hand side of (B·15). The extremal value of σ is

$$\sigma_{\rm ext} = -\frac{|Y_d|}{\lambda}\frac{2(m_{H_2}^2 + m_{\tilde{L}}^2)}{m_{\tilde{Q}}^2 + m_{\tilde{d}_R}^2 + m_{\tilde{L}}^2}, \tag{B·16}$$

and it leads to the stringent constraint as

$$|A_\kappa|^2 \le 9\left[\frac{(m_{\tilde{Q}}^2 + m_{\tilde{d}_R}^2 + m_{\tilde{L}}^2)^2}{4(m_{H_2}^2 + m_{\tilde{L}}^2)}\frac{\lambda^2}{|Y_d|^2} - 2(m_{H_2}^2 + m_{\tilde{L}}^2) + m_S^2\right]. \tag{B·17}$$

B.3. *MSSM CCB-1 direction with gauge singlet*

The MSSM CCB-1 with the gauge singlet direction is the direction along

$$S,\ H_2,\ \tilde{Q},\ \tilde{u}_R,\ \tilde{L} \neq 0. \tag{B·18}$$

The D-term potential along this direction is given by

$$V_D = \frac{1}{6}g_3^2(|\tilde{u}_L|^2 + |\tilde{u}_R|^2)^2 + \frac{1}{8}g_2^2(|\tilde{u}_L|^2 + |\tilde{L}|^2 - |H_2|^2) + \frac{1}{8}g_1^2\left(\frac{1}{3}|\tilde{u}_L|^2 - \frac{4}{3}|\tilde{u}_R|^2 - |\tilde{L}|^2 + |H_2|^2\right)^2. \tag{B·19a}$$

The minimum becomes deeper when the D-term vanishes. By parameterizing the vevs as

$$|\tilde{u}_L| = \alpha|H_2|, \quad |\tilde{u}_R| = \beta|H_2|, \quad |\tilde{L}| = \gamma_L|H_2|, \quad |S| = \sigma|H_2|, \tag{B·20}$$

the D-term vanishes when

$$\alpha^2 + \gamma_L^2 - 1 = 0, \quad \alpha = \beta. \tag{B·21}$$

Along this direction, the potential is given by (23) with

$$\hat{F}(\alpha,\sigma) = \sigma^2(|\lambda|^2 + \sigma^2|\kappa|^2) + |Y_u|^2\alpha^2(\alpha^2+2), \tag{B·22a}$$

$$\hat{A}(\alpha,\sigma) = \alpha^2|A_u||Y_u| + \frac{1}{3}\sigma^3|\kappa||A_\kappa|, \tag{B·22b}$$

$$\hat{m}^2(\alpha,\sigma) = m_{H_2}^2 + \alpha^2(m_{\tilde{Q}}^2 + m_{\tilde{u}_R}^2) + \sigma^2 m_S^2 + (1-\alpha^2)\hat{m}_{\tilde{L}}^2. \tag{B·22c}$$

The constraint for avoiding this minimum is obtained as

$$\left(\alpha^2|A_u||Y_u| + \frac{1}{3}\sigma^3|\kappa||A_\kappa|\right)^2 \le \left[\sigma^2(|\lambda|^2 + \sigma^2|\kappa|^2) + |Y_u|^2\alpha^2(\alpha^2+2)\right] \times \left[m_{H_2}^2 + \alpha^2(m_{\tilde{Q}}^2 + m_{\tilde{u}_R}^2) + \sigma^2 m_S^2 + (1-\alpha^2)\hat{m}_{\tilde{L}}^2\right]. \tag{B·23}$$

This condition cannot be solved analytically and hence the extremal values of α and γ should be determined numerically.

References

1) J. E. Kim and H. P. Nilles, Phys. Lett. B **138** (1984), 150.
2) P. Fayet, Nucl. Phys. B **90** (1975), 104.
3) P. Fayet, Phys. Lett. B **64** (1976), 159.
4) P. Fayet, Phys. Lett. B **69** (1977), 489.
5) P. Fayet, Phys. Lett. B **84** (1979), 416.
6) H. P. Nilles, M. Srednicki and D. Wyler, Phys. Lett. B **120** (1983), 346.
7) J. M. Frere, D. R. T. Jones and S. Raby, Nucl. Phys. B **222** (1983), 11.
8) J. P. Derendinger and C. A. Savoy, Nucl. Phys. B **237** (1984), 307.
9) J. R. Ellis, J. F. Gunion, H. E. Haber, L. Roszkowski and F. Zwirner, Phys. Rev. D **39** (1989), 844.
10) M. Drees, Int. J. Mod. Phys. A **4** (1989), 3635.
11) U. Ellwanger, C. Hugonie and A. M. Teixeira, Phys. Rep. **496** (2010), 1, arXiv:0910.1785.
12) ALEPH Collaboration, DELPHI Collaboration, L3 Collaboration, OPAL Collaboration and The LEP Working Group for Higgs Boson Searches, Phys. Lett. B **565** (2003), 61, hep-ex/0306033.

13) Y. Okada, M. Yamaguchi and T. Yanagida, Prog. Theor. Phys. **85** (1991), 1.
14) H. E. Haber and R. Hempfling, Phys. Rev. Lett. **66** (1991), 1815.
15) J. R. Ellis, G. Ridolfi and F. Zwirner, Phys. Lett. B **262** (1991), 477.
16) R. Barbieri and G. F. Giudice, Nucl. Phys. B **306** (1988), 63.
17) P. H. Chankowski, J. R. Ellis and S. Pokorski, Phys. Lett. B **423** (1988), 327, hep-ph/9712234.
18) P. H. Chankowski, J. R. Ellis, M. Olechowski and S. Pokorski, Nucl. Phys. B **544** (1999), 39, hep-ph/9808275.
19) G. L. Kane and S. F. King, Phys. Lett. B **451** (1999), 113, hep-ph/9810374.
20) M. Bastero-Gil, G. L. Kane and S. F. King, Phys. Lett. B **474** (2000), 103, hep-ph/9910506.
21) G. L. Kane, J. D. Lykken and B. D. Nelson and L.-T. Wang, Phys. Lett. B **551** (2003), 146, hep-ph/0207168.
22) K. Agashe and M. Graesser, Nucl. Phys. B **507** (1997), 3, hep-ph/9704206.
23) A. Brignole, J. A. Casas, J. R. Espinosa and I. Navarro, Nucl. Phys. B **666** (2003), 105, hep-ph/0301121.
24) J. A. Casas, J. R. Espinosa and I. Hidalgo, J. High Energy Phys. **11** (2004), 057, hep-ph/0410298.
25) R. Kitano and Y. Nomura, Phys. Lett. B **631** (2005), 58, hep-ph/0509039.
26) K. Choi, K. S. Jeong and T. Kobayashi and K.-i. Okumura, Phys. Lett. B **633** (2006), 355, hep-ph/0508029.
27) K. Choi, K. S. Jeong, T. Kobayashi and K.-i. Okumura, Phys. Rev. D **75** (2007), 095012, hep-ph/0612258.
28) R. Dermisek and H. D. Kim, Phys. Rev. Lett. **96** (2006), 211803, hep-ph/0601036.
29) H. Abe, T. Kobayashi and Y. Omura, Phys. Rev. D **76** (2007), 015002, hep-ph/0703044.
30) D. Horton and G. G. Ross, Nucl. Phys. B **830** (2010), 221, arXiv:0908.0857.
31) T. Kobayashi, Y. Nakai and R. Takahashi, J. High Energy Phys. **09** (2010), 093, arXiv:1006.4042.
32) J. R. Ellis et al., Phys. Lett. B **176** (1986), 403.
33) G. B. Gelmini, M. Gleiser and E. W. Kolb, Phys. Rev. D **39** (1989), 1558.
34) S. A. Abel, Nucl. Phys. B **480** (1996), 55, hep-ph/9609323.
35) C. F. Kolda, S. Pokorski and N. Polonsky, Phys. Rev. Lett. **80** (1998), 5263, hep-ph/9803310.
36) C. Panagiotakopoulos and K. Tamvakis, Phys. Lett. B **446** (1999), 224, hep-ph/9809475.
37) D. G. Cerdeno, C. Hugonie, D. E. Lopez-Fogliani, C. Munoz and A. M. Teixeira, J. High Energy Phys. **12** (2004), 048, hep-ph/0408102.
38) K. Funakubo and S. Tao, Prog. Theor. Phys. **113** (2005), 821, hep-ph/0409294.
39) D. G. Cerdeno, E. Gabrielli, D. E. Lopez-Fogliani, C. Munoz and A. M. Teixeira, J. Cosmol. Astropart. Phys. **06** (2007), 008, hep-ph/0701271.
40) L. Alvarez-Gaume, J. Polchinski and M. B. Wise, Nucl. Phys. B **221** (1983), 495.
41) C. Kounnas, A. B. Lahanas, D. V. Nanopoulos and M. Quiros, Nucl. Phys. B **236** (1984), 438.
42) M. Claudson, L. J. Hall and I. Hinchliffe, Nucl. Phys. B **228** (1983), 501.
43) M. Drees, M. Gluck and K. Grassie, Phys. Lett. B **157** (1985), 164.
44) J. F. Gunion, H. E. Haber and M. Sher, Nucl. Phys. B **306** (1988), 1.
45) H. Komatsu, Phys. Lett. B **215** (1988), 323.
46) G. Gamberini, G. Ridolfi and F. Zwirner, Nucl. Phys. B **331** (1990), 331.
47) J. A. Casas, A. Lleyda and C. Munoz, Nucl. Phys. B **471** (1996), 3, hep-ph/9507294.
48) T. Kobayashi and T. Shimomura, Phys. Rev. D **82** (2010), 035008, arXiv:1006.0062.
49) Y. Kanehata, T. Kobayashi, Y. Konishi and T. Shimomura, Phys. Rev. D **82** (2010), 075018, arXiv:1008.0593.
50) J. A. Casas and S. Dimopoulos, Phys. Lett. B **387** (1996), 107, hep-ph/9606237.
51) J.-h. Park, Phys. Rev. D **83** (2011), 055015, arXiv:1011.4939.
52) J. Hisano and S. Sugiyama, Phys. Lett. B **696** (2011), 92, arXiv:1011.0260.
53) J. C. Romao, Phys. Lett. B **173** (1986), 309.
54) U. Ellwanger, M. Rausch de Traubenberg and C. A. Savoy, Nucl. Phys. B **492** (1997), 21, hep-ph/9611251.
55) N. K. Falck, Z. Phys. C **30** (1986), 247.
56) D. J. Miller, R. Nevzorov and P. M. Zerwas, Nucl. Phys. B **681** (2004), 3, hep-ph/0304049.

57) D. G. Cerdeno, C. Munoz and O. Seto, Phys. Rev. D **79** (2009), 023510, arXiv:0807.3029.
58) D. G. Cerdeno and O. Seto, J. Cosmol. Astropart. Phys. **08** (2009), 032, arXiv:0903.4677.
59) S. R. Coleman, Phys. Rev. D **15** (1977), 2929 [Errata; **16** (1977), 1248].
60) C. G. Callan Jr. and S. R. Coleman, Phys. Rev. D **16** (1977), 1762.
61) S. R. Coleman and F. De Luccia, Phys. Rev. D **21** (1980), 3305.
62) K.-M. Lee and E. J. Weinberg, Nucl. Phys. B **267** (1986), 181.
63) M. J. Duncan and L. G. Jensen, Phys. Lett. B **291** (1992), 109.